Dryout in a Boiling Channel under Oscillatory Flow Condition*

Hisashi UMEKAWA**, Mamoru OZAWA**,
Akira MIYAZAKI***, Kaichiro MISHIMA****
and Takashi HIBIKI****

Premature dryout due to flow oscillation is a very important factor in designing boiling systems. The flow oscillation depends, in general, on system size and/or configuration, and therefore the relationship between the premature dryout and the flow oscillation has not been fully understood so far. In this investigation, a CHF experiment in a forced flow boiling channel under the oscillatory flow condition has been conducted. Numerical simulation has also been conducted based on the lumped-parameter model of the boiling channel. The simulation well represents the transient behavior of the dryout under the oscillatory flow condition.

Key Words: Critical Heat Flux, Heat Transfer, Flow Oscillation, Lumped-Parameter Model

1. Introduction

Critical heat flux (CHF) in a boiling channel is a very important factor in designing various boiling two-phase flow systems, and therefore many investigations on the CHF under steady flow conditions have been conducted so far.

In boiling channel systems, flow instabilities, such as density wave oscillation, occur under a certain operating condition. Under those flow instability conditions, the CHF correlations based on steady flow conditions may overestimate the CHF value[1)-3)]. These flow instabilities are, however, strongly affected by the system size/configuration, and thus the general relationships between the premature dryout and the flow oscillation are still not well understood so far.

In the previous papers[4),5)], the experimental investigations on the CHF under the forced oscillatory flow condition in a vertical and a horizontal test tubes have been conducted under atmospheric pressure, and the CHF under oscillatory flow condition decreases with the increase in the oscillation amplitude until a certain CHF value which is a function of the oscillation period.

In this paper, the CHF experiment was conducted under oscillatory flow conditions at the pressure up to 0.4 MPa by using three test sections in order to investigate mainly the effect of the tube wall heat capacity, and the numerical simulation was conducted based on the lumped-parameter model.

2. Experimental Apparatus

The experimental apparatus is the forced flow boiling channel system of water shown in Fig. 1, which is mainly composed of a reserve tank of ion-exchanged water, a pump, a plenum, a mechanical oscillator unit, a test section and a separator.

Prior to the experiments, water in the reserve

* Received 7th August, 1995. Japanese original: Trans. Jpn. Soc. Mech. Eng., Vol. 61, No. 583, B (1995), pp. 1048-1054. (Received 29th June, 1994)

** Department of Mechanical Engineering, Kansai University, Yamate-cho 3-3-35, Suita, Osaka 564, Japan
*** Hirakawa Guidom Co., Mikami 2308, Yasu cho, Yasu gun, Shiga 520-23, Japan
**** Research Reactor Institute, Kyoto University, Kumatori cho, Sennan gun, Osaka 590-04, Japan

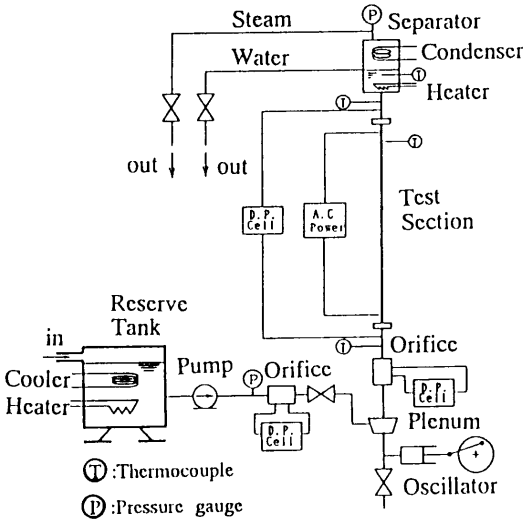

Fig. 1 Experimental apparatus

tank was degassed by boiling. The water was fed into the test section by using the pump of constant discharge with constant inlet temperature, 80 deg.C. The inlet constriction of the valve upstream the plenum was regulated so as not to cause the fluctuation of the mean flow rate from the pump owing to the forced flow oscillation downstream. The mechanical oscillator was composed of a cylinder, a piston and a linkage mechanism, which was able to superimpose a predetermined flow oscillation on a steady flow.

Experiments were conducted by using three SUS 304 tubes with the heated length of 900 mm, and tube diameters were as follow: 3.0 mm I.D. and 4.0 mm O.D. (referred to as 4 mm-Tube), 4.0 mm I.D. and 4.5 mm O.D. (4.5 mm-Tube), and 5.8 mm I.D. and 14.0 mm O.D. (14 mm-Tube). The 14 mm-Tube was heated by Joule heating of D.C. power, and others were heated by Joule heating of A.C. power. The water and vapor were separated at the separator tank. The pressure in this tank was referred to as the system pressure. This system pressure was regulated at the predetermined level by using the heater and the condenser installed in the tank and by adjusting the throttling of outlet valves.

The inlet mass flux of the test section was estimated by the sum of the mean value G_0 which supplied from the pump and the fluctuation component ΔG, and is expressed by $G=G_0+\Delta G\cdot\sin(2\pi t/\tau)$, where τ is a oscillation period.

Experimental range was as follows: the system pressure P was 0.3 and 0.4 MPa. The mean mass flux G_0 was in the range from 100 to 700 kg/m^{2}s, the dimensionless amplitude $\Delta G/G_0$ from 0.18 to 5.53, and the period of the flow oscillation were set at 2.0, 4.0, and 6.0 s. These oscillation periods were determined so as to simulate the density wave oscillation in a steam generator of nuclear reactors and/or small-scale boilers.

In this experiment were measured the outer wall temperatures of test tubes, the inlet and outlet bulk temperatures, the differential pressures across the test section and orifices. The mean mass flux was determined by using the differential pressure across the orifice just downstream the pump. The inlet orifice was installed just upstream the test section. However, owing to the lack of the accuracy of the orifice under the unsteady flow condition, the oscillatory mass flux was not determined by using this inlet orifice, but was calculated on the basis of the piston displacement and oscillation period. The recording trace at the inlet orifice was used for monitoring the phase difference from the temperature traces. The calculated results of the oscillatory discharge from the oscillation unit were within 5% compared with the experimental calibration which was conducted by measuring the oscillation of water level in the transparent glass test tube under pressurized condition.

In this investigation, the CHF value was defined as the heat flux when the outer wall temperature of the tube exceeded beyond 250 deg. C for the 4.0 mm- and 4.5 mm-Tubes and 350 deg. C for the 14 mm-Tube. These temperature thresholds were determined on the basis of the results of the CHF experiment under steady flow conditions, and the difference in the threshold conditions is mainly depend on the difference in the thickness of the tube walls. When the threshold conditions are set at certain different values, the CHF data presented in this paper will be changed accordingly. However, the main discussion in this paper is focused on the macroscopic understanding of the mechanism of the CHF under oscillatory flow condition, and thus the generality in the present discussion is not suffered from the difference in the threshold level.

3. Numerical Simulation

3.1 Simulation model

The numerical simulation was conducted based on the lumped parameter model. In this simulation, at first, the thermal flow behavior in the tube was calculated under an uniform heat flux independently of the wall temperature, i.e. without taking into account the wall heat capacity. Then, the temperature field in the tube wall was calculated based on the thermal flow behavior in the tube. Thus the calculation of the temperature field in the wall does not feedback into the calculation of the thermal flow behavior. This assumption is not serious in the present experimental range, except for the 14 mm-Tube which has rather thick wall and thus the long time constant of

temperature response[5] compared with the period of flow oscillation. In the present stage of investigation, however, the same procedures were adapted throughout the experimental range.

Main assumptions are listed as follows;

(1) Two-phase flow is expressed by the homogeneous flow model.

(2) The system pressure is constant.

(3) The flow is thermally equilibrium.

(4) The specific volumes of subcooled liquid and superheated vapor are constant, and are equal to those of the saturated liquid and vapor, respectively.

(5) The heat flux is uniform along the tube and is constant in the calculation of the thermohydraulics of water.

(6) The heat loss from the test section to the ambient air is ignored.

(7) The axial heat conduction through the tube wall is not took into account.

(8) Physical properties of the tube material are constant.

(9) The radial temperature gradient in the tube material during the transients is the same as that under steady state condition.

In this investigation, the experimental range included the large amplitude oscillation which induced the flow reversal. Under such flow reversal condition, the first assumption may not be accurate. Owing to the lack of the sufficient information as well as suitable constitutive equations during the flow reversal transients, the first assumption is, however, reasonably applied to the present simulation at this stage of research, which will make it possible to construct the simulation model for the CHF phenomena under density wave oscillations consistently using the same model.

3.2 Numerical simulation method

In the numerical simulation, at first, the flow field was calculated using next one-dimensional conservation equations. The calculation method is almost the same as that was used for the analysis of the density wave oscillation under the natural circulation loop of liquid nitrogen[6],[7]. Therefore only the main part and the difference from the previous ones[6],[7] are described in this section

Mass conservation:

$$\frac{\partial \rho}{\partial t}+\frac{\partial}{\partial z}(\rho u)=0 \qquad (1)$$

and energy conservation:

$$\frac{\partial}{\partial t}(\rho h)+\frac{\partial}{\partial z}(\rho h u)=q_V \qquad (2)$$

where ρ represents the density, t the time, z the axial coordinate, u the velocity, h the specific enthalpy, and q_V represents the volumetric heat flux. The first term in Eq.(2) is an approximation of the internal energy, which is a usual way of simulation of a boiling channel.

The simulation model of the boiling channel is shown in Fig. 2. The test section is divided, in principle, into three regions: the subcooled liquid region, the two-phase region and the superheated vapor region. On the basis of the assumptions(2), (3) and (4), the distributions of the velocity u, specific volume v and specific enthalpy h were expressed as shown in Fig. 2, where L_T represents the test section length, subscripts L and G the saturated values of liquid and vapor, subscripts IN and EX represent the values at the inlet and outlet of the test section, respectively. On the basis of such distributions of various variables, ordinary differential equations were obtained by integrating these conservation equations over each region. Solving Eq.(2), the velocity gradient in the two-phase region is given by;

$$\frac{du}{dz}=q_V\frac{v_{LG}}{h_{LG}} \qquad (3)$$

where h_{LG} is the latent heat and v_{LG} is the specific volume difference between vapor and liquid phases.

The integration of Eq.(2) over the subcooled liquid region gives the boiling boundary λ_L movement, where the Leibniz rule is adapted.

$$\frac{d\lambda_L}{dt}=2u_{IN}-\frac{2q_V\lambda_L}{\rho_L(h_L-h_{IN})} \qquad (4)$$

The superheated boundary λ_G is obtained by the integration of Eq.(1) over the two-phase region.

$$\frac{d\lambda_G}{dt}=\frac{\rho_{TP}\rho_L}{\rho_{TP}-\rho_G}\frac{d\lambda_L}{dt}-\frac{\rho_G u_{EX}-\rho_L u_{IN}}{\rho_{TP}-\rho_G} \qquad (5)$$

where ρ_{TP} is the integral-averaged density of two-phase region, and is defined as follows;

$$\rho_{TP}=\frac{\ln(v_G/v_L)}{v_G-v_L} \qquad (6)$$

Under the condition without the superheated vapor region, the specific volume at the exit v_{EX} is calculated by integrating Eq.(1) over the two-phase region, as follows;

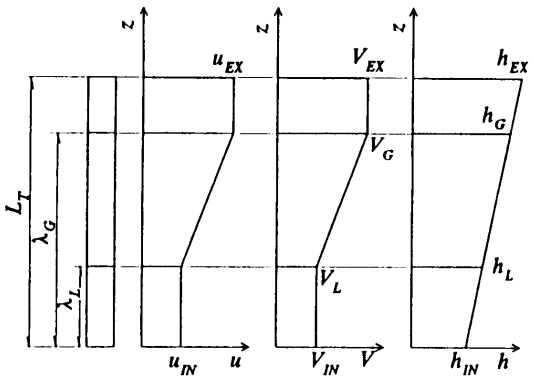

Fig. 2 Simulation model

$$\frac{dv_{EX}}{dt}=\frac{\frac{u_{IN}}{v_L}-\frac{u_{EX}}{v_{EX}}-\left[\frac{1}{v_L}-\frac{ln\,(v_{EX}/v_L)}{v_{EX}-v_L}\frac{d\lambda_L}{dt}\right]}{\frac{L_T-\lambda_L}{(v_{EX}-v_L)^2}\left(1-\frac{v_L}{v_{EX}}\ln\frac{v_{EX}}{v_L}\right)} \quad (7)$$

The thermal flow behavior was calculated from these ordinary differential equations by using Runge-Kutta method under uniform heat flux condition.

The next stage of the simulation is the calculation of the wall temperature transients. The heat conduction equation in radial direction is expressed by Eq.(8),

$$\frac{\partial T}{\partial t}=\frac{k}{C_{PT}\rho_T}\left[\frac{1}{r}\frac{\partial}{\partial r}\left(r\frac{\partial T}{\partial r}\right)\right]+\frac{q_T}{C_{PT}\rho_T} \quad (8)$$

where T represents the temperature, k the thermal conductivity of the tube material, r the radial coordinate, and q_T is the volumetric heat generation rate of the tube. On the basis of the assumption(9), the integration of Eq.(8) across the tube wall gives the mean wall temperature T_M in the radial direction as follows;

$$\frac{dT_M}{dt}=\left(\frac{-2r_1q_s}{r_0^2-r_1^2}+q_T\right)\Big/C_{PT}\rho_T \quad (9)$$

where q_s is the heat flux at the inner surface of the tube. In the calculation of q_s, the bulk temperature of the working fluid was the saturation temperature in the two-phase and superheated vapor regions, and the bulk temperature in the subcooled liquid region was calculated under the assumption of the thermodynamic equilibrium. The assumption of the constant bulk temperature in the superheated vapor region was used for overcoming the difficulty in the flow reversal transients. The heat transfer coefficients were given by Dittus-Boelter's equation[8] in the subcooled liquid and the superheated vapor regions, and by Steiner's correlation[9] in the two-phase region. The time step for calculation was set at 0.01 s in the present simulation.

4. Results and Discussion

4.1 CHF under steady flow condition

Examples of CHF data under the steady flow condition are plotted in Fig. 3, where the same dimensionless coordinate system as Mishima[3] is used. The broken lines in Fig. 3 correspond to the conditions of constant exit qualities, $X_{eq}=1$ and 0. The correlations of Katto[10] and Macbeth[11] are drawn by solid and dot-dash lines, respectively. The CHF data under the steady flow condition approximately agree with these correlations. These experimental data correspond to Katto's L-regime at lower mass flux and to the transition region from L to H-regimes at higher mass flux.

4.2 CHF under oscillatory flow condition

4.2.1 Recording traces Figure 4 shows one of the experimental recording traces: the wall temperatures T_o, the differential pressure across the test tube D.P. and the differential pressure at the orifice just upstream the test tube. Wall temperatures were measured at the exit, at 50 mm and 450 mm upstream the test tube exit. The differential pressure at the inlet orifice corresponds to the inlet velocity G, and therefore the scale unit is converted to the mass flux unit. The arrows in Fig. 4 represent the synchronized time among the various traces.

The radiation heat transfer and the heat conduction from the electrode make the exit wall temperature lower than that at 50 mm from the exit. Thus the CHF was detected by the temperature at 50 mm upstream from the exit of the test section. The drastic decrease in the pressure drop is followed by the rapid increasing in the wall temperature, and the

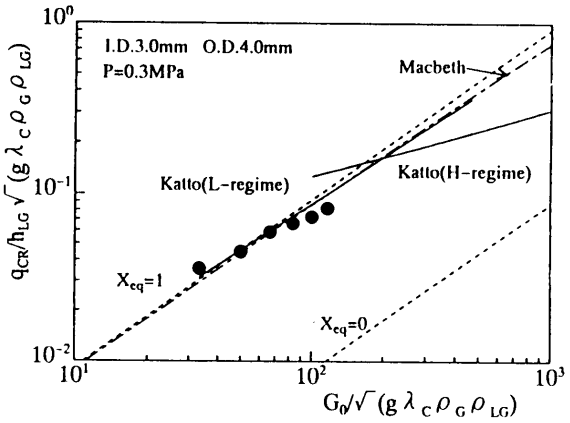

Fig. 3 CHF under steady flow condition

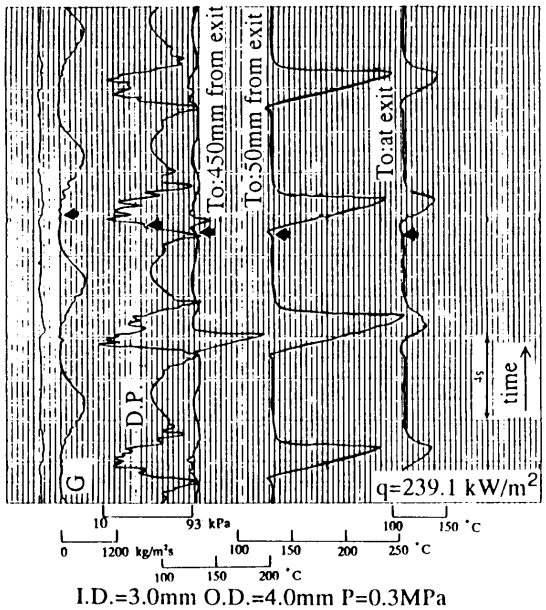

Fig. 4 Typical recording trace under oscillatory flow condition

wall temperature decreases quickly when the inlet mass flux approaches the maximum value.

The simulation result under the same condition as in Fig. 4 is shown in Fig. 5 with reference to the exit and the inlet velocities u_{EX} and u_{IN}, the exit specific volume v_{EX}, the wall temperature T_o (at the test section exit) and the differential pressure DP. The differential pressure is drawn by the solid line, but with the three components: the acceleration DPA, the friction DPF and the gravity terms DPG are shown as the distances between the solid, broken and dotted lines. The simulation result gives a qualitative agreement with the experimental result.

On the basis of the simulation result, the dryout behavior is postulated as follows: the exit-velocity fluctuation has a certain delay to the inlet-velocity fluctuation. Moreover, the relationship between two fluctuations depends strongly on the vapor generation rate in two-phase region, which leads to the relaxation-type oscillation at the exit even in the case of sinusoidal oscillation at the inlet. Approaching to the minimum value of u_{IN}, the subcooled length begins to decrease and the vapor generation rate increases owing to the decrease in the mass flux. These behavior cause rapid ejection of two phase mixture from the test section, which is represented by the rapid increase in v_{EX} and u_{EX}, and is followed by the rapid decrease in the pressure difference. Then the exit quality exceeds unity, i.e. superheated vapor region appears at the exit of the tube. This superheated region extends upstream with time until the next increase in u_{IN}. During the appearance of this superheated region, the heat transfer at the inner wall retains very low level compared with that in the two-phase region. Then the wall temperature increases until the rewetting owing to the increase in the inlet velocity.

These behavior mentioned above was the case observed under relatively large-amplitude condition. On the other hand under relatively small-amplitude condition, the rapid decrease in differential pressure following to the rapid ejection of two-phase mixture was not observed, while the rather slow transients are observed in the appearance of the superheated vapor region.

4.2.2 Critical heat flux Experimental results of the CHF under the oscillatory flow conditions are shown in Fig. 6 with the simulation results. The CHF in the simulation was decided by the same threshold condition as in the experiment. The experimental data of CHF decreases with increasing the normalized amplitude $\Delta G/G_0$, and has a saturation tendency toward a certain level which is determined uniquely by the oscillation period. The simulation results show good agreements with the experimental results.

The rapid increase in the wall temperature occurs during the dryout period (cf. Fig. 5), therefore this period may strongly affect on the CHF. Figure 7 shows the critical dryout period, i.e. the dryout period at the tube exit during the CHF condition obtained in

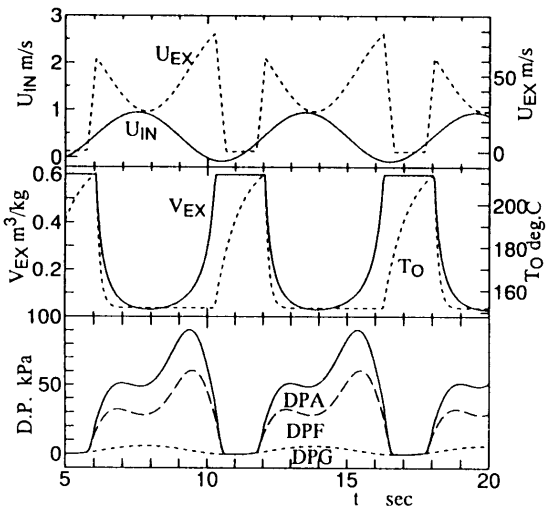

Fig. 5 Simulation results

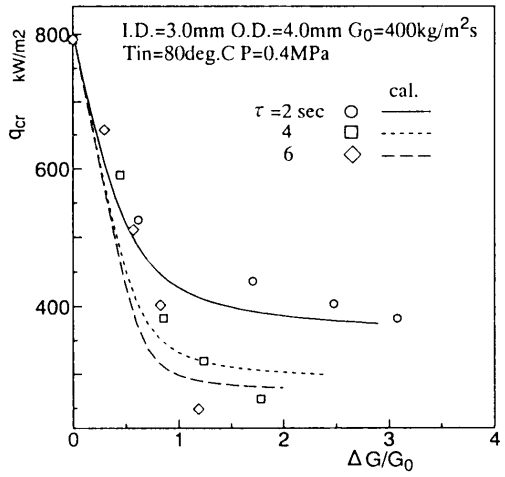

Fig. 6 CHF under the oscillatory flow condition

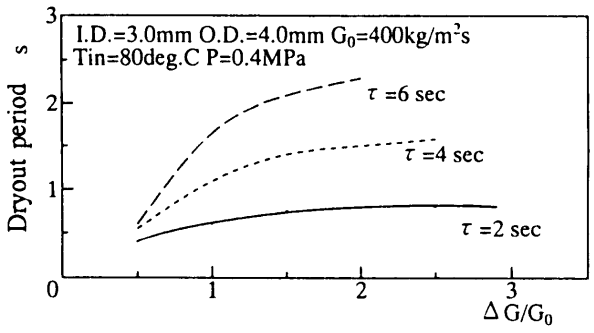

Fig. 7 Simulation results of the dryout period at the tube exit

the simulation. The increase in the amplitude causes the increase in the dryout period. The longer dryout period causes the larger temperature rise during the dryout, and therefore the increase in the amplitude results in the decrease in the CHF. The dryout period is limited to the half of the oscillation period, so that the CHF under oscillatory flow condition have a saturation value which depends on the oscillation period.

In Fig. 8, the CHF tendencies are the same as those of Fig. 7, and the calculation results also show good agreement with experimental results. But in this case the simulation overestimates the CHF for the small amplitude oscillation, and the differences between the simulation and the experimental results decrease with the increase in the oscillation amplitude. These facts suggest that the CHF condition in the case of small amplitude relative to the mean mass flux is essentially induced by the similar mechanism as in the steady state experiment ; but the CHF under the large amplitude oscillation may be dominated not only by a microscopic flow structure such as liquid film instability and entrainment generation but also by a macroscopic transients of the superheat boundary and the wall heat capacity due to the enhancement of mechanical and thermodynamic equilibrium.

Figures 9 to 11 show influence of the mass flux, the system pressure and the heat capacity of the tube wall on the CHF, respectively. In these figures the vertical coordinate is the CHF ratio normalized by the CHF value under the steady flow condition. The reduction of the CHF ratio at large mass flux is larger than that at small mass flux. This is owing to the difference in the heat flux. The large heat flux is required by the dryout at large mass flux, and then the rising rate of the wall temperature increases with the increase in the heat flux. This reason is also applied to the influence of the pressure difference shown in Fig. 10. As the inlet water temperature is constant

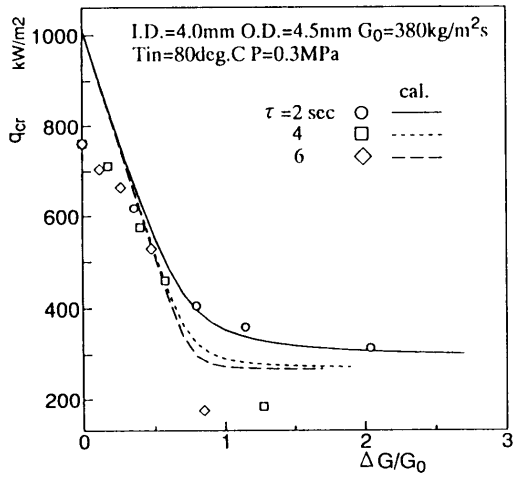

Fig. 8 CHF under the oscillatory flow condition

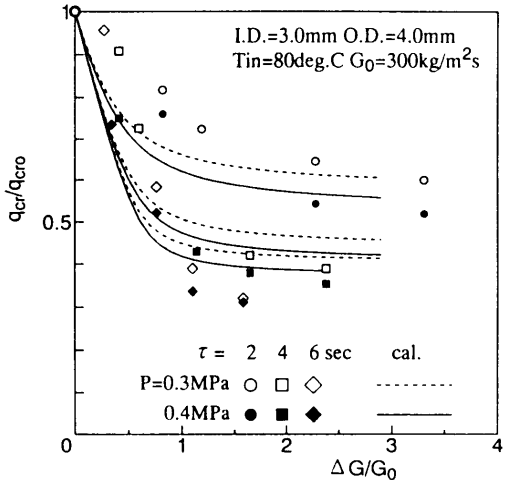

Fig. 10 Influence of the system pressure on the CHF

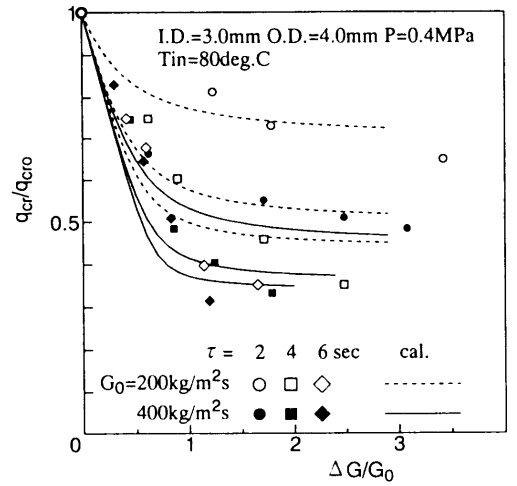

Fig. 9 Influence of the mean mass flux on the CHF

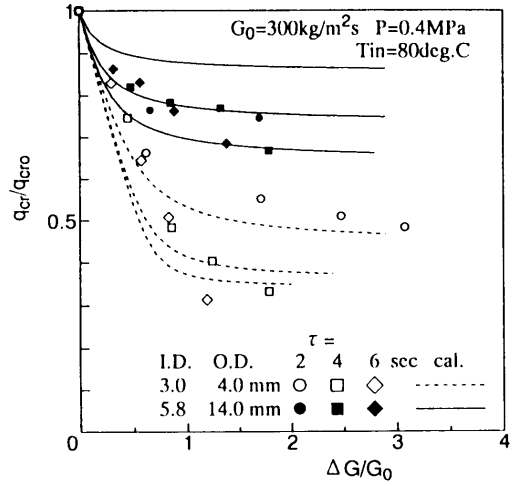

Fig. 11 Influence of the tube wall heat capacity on the CHF

throughout this investigation, the CHF at $P=0.4$ MPa is slightly larger than that at $P=0.3$ MPa, which makes the larger reduction of the CHF ratio at 0.4 MPa compared with that at 0.3 MPa.

Figure 11 shows the influence of the tube wall thickness on the CHF. The reduction of the CHF ratio of the large heat capacity tubes is smaller than that of the small heat capacity tubes. The difference in the oscillation period on the CHF ratio becomes less significant with increasing the tube wall heat capacity. These tendencies depend on the delay time in the transient behavior of the wall temperature. For the tube with large heat capacity, the present simulation shows relatively poor agreement with the experimental result. This poor agreement depends probably on the present method of simulation, i.e. the calculation of the flow dynamics is conducted under the uniform heat flux distribution only with taking into account the dynamic interaction from the flow to the wall temperature dynamics but without the feedback from the wall to the flow.

5. Conclusion

The experimental and numerical investigations on the CHF under oscillatory flow condition were conducted. The numerical simulation based on the lumped-parameter model represented well the transient behavior of the dryout for the tubes with relatively small heatcapacity. The heat flux distribution and its dynamics have to be took into account in simulating the CHF for tubes with large heat capacity.

Acknowledgments

This investigation was supported in part by the Grant-in-Aid for Scientific Research of the Ministry of Education, Science and Culture of Japan, No. 05650217 (1993, 1994), and was carried out in part under the Visiting Researcher's Program of the Research Reactor Institute, Kyoto University (No. 5007). The authors wish to express their sincere thanks to Messrs. M. Kataoka and M. Miyoshi.

References

(1) Sato, T., Hayashida, Y. and Motoda, T., The Effect of Flow Fluctuation on Critical Heat Flux, Proc. 3rd Int. Heat Transf. Conf., Chicago, Vol. 4(1966), p. 226.

(2) Bergles, A.E., Lopina, R.F. and Fiori, M.P., Critical-Heat-Flux and Flow Pattern Observations for Low-Pressure Water Flowing in Tubes, Trans. ASME, J. Heat Transf., Vol. 89(1967), p. 69.

(3) Mishima, K., Nishihara, H. and Michiyoshi, I., Boiling Burnout and Flow Instabilities for Water Flowing in a Round Tube under Atmospheric Pressure, Int. J. Heat Mass Transf., Vol. 28, No. 6(1985), p. 1115.

(4) Ozawa, M., Umekawa, H., Yoshioka, Y. and Tomiyama, A., Dryout under Oscillatory Flow Condition in Vertical and Horizontal Tubes, Int. J. Heat Mass. Transf., Vol. 36, No. 16(1993), p. 4076.

(5) Ozawa, M. and Umekawa, H., Experimental Investigation on Dryout under Oscillatory Flow Condition in Vertical and Horizontal Tubes, Proc. German-Jpn. Symp. Multiphase Flow, Karlsruhe, KfK 5389(1994), p. 227.

(6) Asao, Y. Ozawa, M. and N. Takenaka, Circulation Characteristics and Density Wave Oscillation in a Natural Circulation Loop of Liquid Nitrogen, (in Japanese), Jpn J. Multiphase Flow, Vol. 6, No. 2(1992), p. 159.

(7) Ozawa, M. Asao, Y. and Takenaka, N. (Gouesbet, G. and Berlemont, A., eds.), Density Wave Oscillation in a Natural Circulation Loop of Liquid Nitrogen, Instabilities in Multiphase Flows, (1993), p. 113, Plenum Press.

(8) Ueda, T., Two-phase flow, (in Japanese), (1981), p. 252, Yokendo Pub.

(9) D. Steiner, VDI-Wärmeatlas (4-Auflage), (1984), Hbb 1-29, VDI Verlag.

(10) Katto, Y., Critical Heat Flux, Advances in Heat Transfer, 17(1985), p. 2, Academic Press.

(11) Ueda, T., Two phase flow, (in Japanese), (1981), p. 290, Yokendo Pub.